Mineralogia, vol. 54, 2023, 18-30 *Original Paper*

DOI: 10.2478/mipo-2023-0003

Synthetic zeolite derived from coal fly ash decorated with magnetic alginate bead: Application to detoxification of arsenic and vanadium

Eugeniusz Swistun[1], Maciej Sobczyk[1], A. Santhana Krishna Kumar[1,2], Wei-Lung Tseng[2,3], Tomasz Bajda[1]*

[1]Faculty of Geology, Geophysics and Environmental Protection, AGH University of Science and Technology, Al. Mickiewicza 30, 30-059, Krakow, Poland
[2]Department of Chemistry, National Sun Yat-sen University, No. 70, Lien-hai Road, Gushan District, Kaohsiung 80424, Taiwan
[3]School of Pharmacy, Kaohsiung Medical University, No. 100, Shiquan 1st Road, Sanmin District, Kaohsiung 80708, Taiwan

*Corresponding author: bajda@agh.edu.pl

Abstract

Heavy metal toxicity is highly demanding and challenging to clean up the pollutants. To recover the issues mentioned above, we propose a hydrothermal synthesis of zeolite (NaX-UP). Further surface modification by poly-ethylenimine (PEI) could turn to be amine-modified zeolite nanosheets (zeolite NSs) possessed plenty of hydroxyl and amino groups (Al-O, Si-O-Si, Si-OH and NH_2) on their surface, decorated with magnetic nanoparticles (Fe_3O_4 NPs), that are enabled to bridge with inter and intramolecular hydrogen bonding an additionally electrostatic interaction might be a significant role. Further, this can be converted into magnetic bead crosslinking with sodium alginate immersed in an excess calcium chloride solution. The-as formed Fe_3O_4 NPs decorated amine modified zeolite alginate bead denoted to be (Fe_3O_4 NPs decorated @PEI-zeolite NSs alginate bead) upholding a significant advantage would aim to clean up the anionic pollutants are [As(V) & V(V)] from an aqueous solution.

Keywords: Fly ash, zeolite, magnetic nanoparticle, alginate bead, electrostatic interaction, heavy metal sorption

1. Introduction

Groundwater is one of the primary sources of drinking water consumption for large groups of people around the globe (Han et al. 2019). Amplified arsenic (As) concentrations are prime pollution for groundwater poisoning. As a result, a massive group of people were affected by consuming arsenic-contaminated water (Suazo-Hernandez et al. 2019). Subsequently, arsenic is released into the environment, mainly through the geothermal process of volcanic emissions and anthropogenic activities such as the combustion of fossil fuels (Han et al. 2019; Suazo-Hernandez et al. 2019). Arsenic exists in various forms of inorganic oxyanions such as arsenite [As(III): H_3AsO_3 and $H_2AsO_3^-$] and arsenate [As(V): $H_2AsO_4^-$, $HAsO_4^{2-}$, and AsO_4^{3-}] (Yang et al. 2022). Hence, these arsenic species can readily assimilate into the human system. Further, this could lead to severe damage, such as oncogenic diseases, endocrine infections, and respiratory and cardiovascular impair (Abdellaoui et al. 2021). To keep the above consideration, the World Health Organization (WHO) suggests that the admissible limit of arsenic in drinking water must be 0.01 ppm (Yang et al. 2019). Vanadium(V) is primarily utilized in industrial purposes for manufacturing metallurgical needs such as glass, textile, ceramic, rubber industries, oil refineries, developing photographic units from the pigments sector, and power plant units utilizing vanadium-rich in coal (Mthombeni et al. 2018). Consequently, those industrial activities discharge significant amounts of vanadium-contaminated water that greatly damage

groundwater pollution. Vanadium exists in most stable forms are tetravalent [V(IV)] and pentavalent [V(V)] ion (Mthombeni et al. 2016), the penta-valent V(V) are more stable and toxic than the tetravalent V(IV) (Salehi et al. 2020). Hence, Vanadium V(V) generally exists in the form of VO_2^+, $H_2VO_4^-$ and HVO_4^{2-} depending on their solution pH. Vanadium can easily enter the human system through the food chain of polluted water consumption. Further, this could lead to damaging breathing disorders, paralysis and adverse effects on the dysfunction of the liver and kidneys (Salman et al. 2017). To protect human health, the mandatory surface water discharge their limit must be regulated into 0.2 ppb of V, as proposed by the United States Environmental Protection Agency (US-EPA) (Kong et al. 2020). So, therefore it's essential to treat vanadium contaminations before discharge into the environment.

Arsenic and vanadium engrossed elevation toxicity, which is primarily affected, leading to numerous illnesses and severe ecological complications. In terms of multiple intoxication technologies that have been investigated so far, for instance, coagulation, ion exchange, membrane filtration, and biological/chemical reduction are numerous techniques that are mainly involved, but in elevation operating and maintenance costs, enormous sludge creation, and practice of hazardous chemicals rigorously limit their an extensive applications, among them conventional process for sorption techniques are preferred because of their cost-effective (Mthombeni et al. 2018; Yang et al. 2019; Abdellaoui et al. 2021; Yang et al. 2022). Recently, remediation through sorption techniques have been widely recognized due to their sustainable implementations, including their regeneration and multiple times reuse of the solid support (adsorbent). Those enlarged performance for sorption materials are mainly involved such as activated carbon, clay minerals, graphene oxide, and synthetic zeolite sorbent, which can be derived from coal fly ash (Mthombeni et al. 2018), synthetic zeolite, which are mainly consisting of a combination of tetrahedral $[SiO_4]^{4-}$ and $[AlO_4]^{4-}$ joined by oxygen atoms, these main functional groups are from zeolite such as aluminous (=Al-OH) and silanols (=Si-OH), which are ionized as a function of pH. Hence, due to their isomorphic substitution of Si^{4+} and Al^{3+}, this alumino silicate has permanent negative charges which are balanced by monovalent or divalent cations dissolved in the aqueous medium (Mthombeni et al. 2018; Han et al. 2019; Suazo-Hernandez et al. 2019; Abdellaoui et al. 2021; Yang et al. 2022). The hydrated cations (Na^+, Ca^{2+}) are attracted to the alumina silicates, imparting high cation exchange capacity (CEC) to create zeolite networks.

The as-developed zeolite is commonly used to remove divalent cations (Pb^{2+}, Cu^{2+}, and Cd^{2+}) from contaminated waters because of their permanent negative charge and also, CEC favors' their sorption of cations rather than anionic species (Han et al. 2019; Suazo-Hernandez et al. 2019; Yang et al. 2022). Synthetic zeolite can be obtained in two different routes; in the first one, alkaline fusion takes place at high temperatures followed by hydrothermal treatment; the second method is a direct hydrothermal treatment which is not preferable mostly (Yang et al. 2019; Abdellaoui et al. 2021). So far, several researchers were reported that synthetic zeolite could be efficiently applied for the sorption of heavy metals (Yang et al. 2019) from aqueous systems. These synthetic zeolite have been found for various applications due to their simple regeneration, low cost, environmental-friendly material an excellent thermal stability, higher cation-exchange capacity and enlarged surface area (Han et al. 2019). However, the unmodified zeolites have negative charges on their framework, owing to their lower sorption ability of anionic contaminations such as negatively charged inorganic/organic pollutants. In previous studies, the sorption capacity performance of unmodified zeolite for removing anionic contaminations is minimal (Han et al. 2019; Yang et al. 2019).

To enhance their sorption performance, here we propose that the modification of synthetic zeolite with amine rich moiety of (polyethyleneimine, PEI), in acidic pH these protonated amino functional groups (-N,-NH and $-NH_2$) electrostatically bind with negatively charged (OH^-) hydroxyl groups on their surface of zeolite acts as a suitable sorbent for sorption of anionic pollutants (Han et al. 2019; Suazo-Hernandez et al. 2019; Yang et al. 2022) due to their interesting interactions such as hydrogen bonding and electrostatic interaction. For example, Mthombeni et al. (2016, 2018) have synthesized a poly-pyrrole (Ppy) functionalized meso-porous zeolite as a template. However, these reported synthetic zeolite-based sorbents have shown a minimal potential to remove vanadium. However, their adsorption capacity needs considerable enhancement. It's worth mentioning that the maximum adsorption capacity values of those above-discussed adsorbents were reported to be 10 to 72 mg g^{-1} for arsenic (V) (Han et al. 2019; Suazo-Hernandez et al. 2019; Yang et al. 2019, 2022; Abdellaoui et al. 2021), 12 to 277 mg g^{-1} for vanadium (V) (Mthombeni et al. 2016, 2018; Salman et al. 2017; Kong et al. 2020; Salehi et al. 2020) in sequence. To overcome the issues mentioned above, magnetic (Fe_3O_4) nanoparticles (NPs) have attracted worldwide attention due to their sorption abilities for various heavy metals. These magnetic NPs possess magnetic behavior, which allows their easy separation from an aqueous solution through a simple magnetic sorption process. Nevertheless, these magnetic NPs are challenging to use in continuous-flow systems due to their small particle size and instability. They are highly susceptible to oxidation when exposed to the atmosphere, either.

To overcome these difficulties, it's possible to disperse and cross-link NPs by functionalized porous material of PEI-modified zeolite. As many other authors are claimed sucessively, the resulting Fe_3O_4 NPs decorated PEI-modified zeolite have a high surface area and enhanced adsorption capacity and are highly stable and resistant to strong acids (Han et al. 2019; Suazo-Hernandez et al. 2019; Yang et al. 2022). The modification of synthetic zeolite with magnetic nanoparticles (Fe_3O_4 NPs) not only increases their sorption capacity but also improves their physicochemical properties of zeolite, such as high

specific surface area, porosity, and thermal stability for more effective sorbent in real wastewater treatment (Mthombeni et al. 2016; Suazo-Hernandez et al. 2019). Nevertheless, these Fe_3O_4 NPs modified zeolite-based nanomaterials possess good sorption capacity due to their great ratio of surface to volume and enlarged surface area. Recently, a few studies are reported that magnetite NPs coated with synthetic zeolite surface, the as-made sorbent was able to effectively capture As(V) from an aqueous systems (Suazo-Hernandez et al. 2019; Abdellaoui et al. 2021; Yang et al. 2022). Additionally, magnetic NPs were modified zeolite surfaces, and the as-made sorbent effectively removed V(V) up to 74.9 mg g^{-1} from aqueous systems (Mthombeni et al. 2016). However, these reported hybrid nano-materials (Mthombeni et al. 2016; Suazo-Hernandez et al. 2019; Abdellaoui et al. 2021; Yang et al. 2022), possess very low sorption efficiency.

To overcome the above shortage, to enhance their adsorption performance, we propose that magnetic NPs decorated PEI-modified zeolite were cross-linked by alginic acid in an excess amount of calcium chloride and efficiently fabricated. The as-prepared magnetic alginate bead-based adsorbent has great porosity and a larger surface area to volume ratio (Suazo-Hernandez et al. 2019). These features might enhance their surface behaviors of the adsorbent due to their removal capability can be improved tremendously (Mthombeni et al. 2016, 2018). The as-developed adsorbent (Fe_3O_4 NPs decorated PEI modified zeolite alginate bead) would aim to clean up the hazardous pollutants are As(V) and V(V) in an aqueous medium.

2. Details of Experimental

2.1. Materials and Procedures

Sodium meta arsenate ($NaAsO_3$), sodium vanadate ($NaVO_3$) were obtained from Sigma-Aldrich (St Louis, MO, USA). Poly ethylenimine, PEI M.W., 750 kDa, were procured from Alfa-Aesar (Ward Hill, MD, USA). The alginic acid sodium salt, $CaCl_2$, NaOH, KOH, NH_4OH, HCl, $FeCl_2{\cdot}4H_2O$, and $FeCl_3{\cdot}6H_2O$ were obtained from Chem-pure chemicals (Krakow, Poland). All other reagents were purchased from analytical grade without further purification, and double distilled water was used throughout the experiments.

2.2. Synthesis of Zeolite derived from coal fly ash

For hydrothermal synthesis, 10 g of fly ash samples were mixed with 12 g of NaOH, and the resulting mixture was heated up to 823 K for 60 minutes (Kunecki et al. 2021). After cooling to room temperature, sodium aluminate was slowly added into the grinded mixture to control their molar ratio of SiO_2/Al_2O_3. Subsequently, the as obtained mixture was further magnetically agitated at room temperature for 16 hours and then temperature was raisin up to 373 K for another 24 hours (Amoni et al. 2022). After cooling down to room temperature, the suspension was filtered, and then the solid product was repetitively washed with 1 L of deionized water and dried up 378 K for 16 hours. Figure 1 shows detailed synthetic processes of zeolite (NaX-UP) derived from coal fly ash are demonstrated (Izidoro et al. 2013; Kunecki et al. 2021; Amoni et al. 2022). The main chemical compositions are as follows: silica, alumina, sodium, and other components as shown in Table 1, these elemental compositions were confirmed by X-ray fluorescence techniques.

2.3. Synthesis of amine-modified Zeolite NSs (PEI-Zeolite NSs)

A known amount of 1.0 g of zeolite (NaX-UP) was immersed in 150 mL of de-ionized water and 10 mL of PEI (10 % V/V, 20 mg mL^{-1}). The resulting mixture was homogeneously stirred for 10 hours (Mthombeni et al. 2016, 2018; Santhana Krishna Kumar et al. 2022), and the terminal amino group from PEI functionalization through their electrostatic interaction with negatively charged zeolite surface of silanol (Si-OH and Al-OH) groups. After separating their supernatant solution, the as obtained solid compound was denoted to be (PEI modified zeolite NSs).

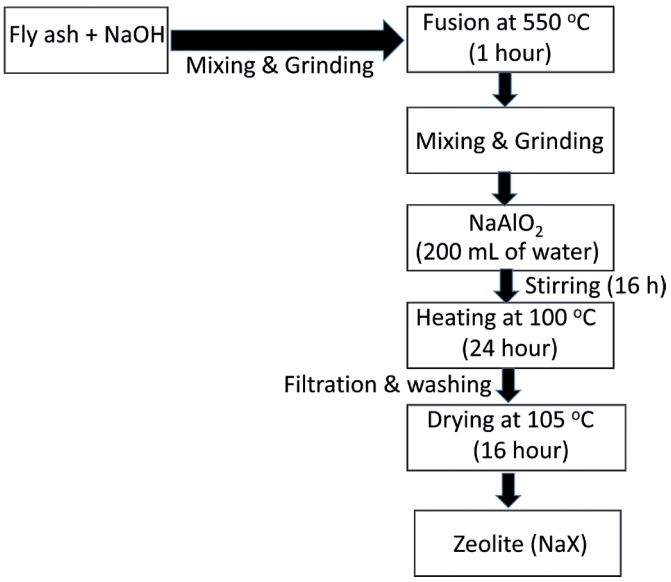

Figure 1. Schematic illustration about the synthesis of zeolite NaX-UP.

Table 1. Elemental compositions determined by XRF method.

S. No.	Composition	XRF [% weight]
1	SiO_2	32.05
2	TiO_2	0.04
3	Al_2O_3	27.07
4	Fe_2O_3	0.40
5	MnO	0.08
6	MgO	1.16
7	CaO	5.32
8	K_2O	0.52
9	Na_2O	8.81
10	P_2O_5	0.07
11	SO_3	0.10
12	LOI	24.19
	Σ	99.81

2.4. Synthesis of bare Fe_3O_4 NPs and Fe_3O_4 NPs decorated on their surface of PEI-zeolite NSs

Initially, PEI-modified zeolite NSs (0.3 g) were dispersed in DD water (120 mL), followed by $FeCl_2 \cdot 4H_2O$ (7.2 g) and $FeCl_3 \cdot 6H_2O$ (2.8 g), were gradually mixed with the obtained mixture was stirred at 80°C for 30 minutes, the resulting solution was deoxygenated by bubbling with argon gas for 30 minutes, followed by quick injection an ammonia solution (15 mL, 4 M), the entire solution turned to be a dark black color suspension which confirmation that, Fe_3O_4 NPs were strongly bonded with the surface of PEI modified zeolite NSs, the-as obtained solution was further brought down to ambient temperature and then rinsed multiple times with DD water (Santhana Krishna Kumar et al. 2022). For comparison, a control experiment was subjected into prepare bare Fe_3O_4 NPs. As mentioned above, the synthetic route was followed without adding PEI-zeolite NSs.

To prepare magnetic alginate bead (adsorbent), a known amount of alginic acid 2.0% w/v was individually mixed with 30 mg mL^{-1} of different nanomaterials such as PEI-zeolite NSs, bare Fe_3O_4 NPs and PEI-zeolite NSs@ Fe_3O_4 NPs were slowly stirred at 80 °C for 2 hours to get the homogeneous solution, the as-prepared alginic acid modified nanomaterials were gradually dropping into 3.0 % w/v of $CaCl_2$ solution and kept for crosslinking 24 hours to obtain their homogeneous well-shaped calcium cross-linked PEI-zeolite NSs modified alginate beads and Fe_3O_4 NPs decorated PEI modified zeolite NSs alginate beads are displayed in (Figures 2A and B), which are turned to be great flexibility. Furthermore, the schematic illustration of the functionalization procedure is depicted in Figure 3**.**

2.5. Batch sorption studies for heavy metals

Batch adsorption studies were systematically assessed by monitoring various pH, temperature and known amounts of adsorbent (2000 mg). The adsorption isotherm studies were established by increasing their heavy metals initial concentration ($C_{initial}$) varied from 10 to 500 mg mL^{-1} for As (V) and V (V). Similarly, the kinetics studies were also conducted by varying their contact time between 0 to 240 mins intervals at fixed concentrations of heavy metals, pH and adsorbent doses (Kalidhasan et al. 2012; Santhana Krishna Kumar et al. 2013, 2022). After the metal ions' successful adsorption, the supernatant solution was free of As(V) and V(V). Moreover, the unabsorbed (C_e) (supernatant) metal ions concentrations were determined by ICP-MS techniques (Santhana Krishna Kumar et al. 2022). The amount of

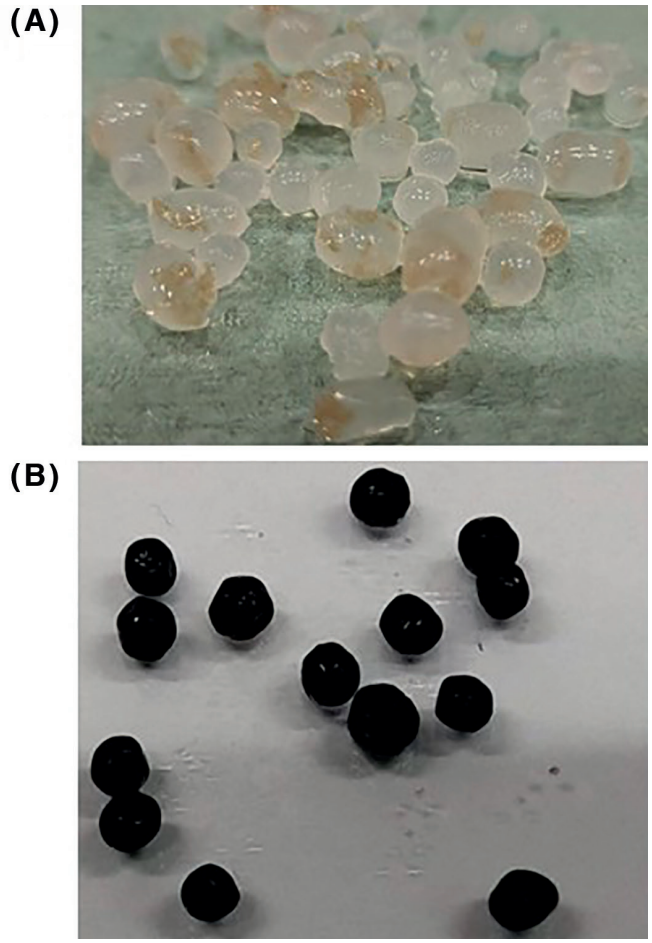

Figure 2. As shown in (A) PEI-zeolite NSs alginate bead (dusky and colorless), (B) the bare Fe_3O_4 NPs were decorated on their surface of PEI-zeolite NSs alginate bead (magnetic alginate bead, black color).

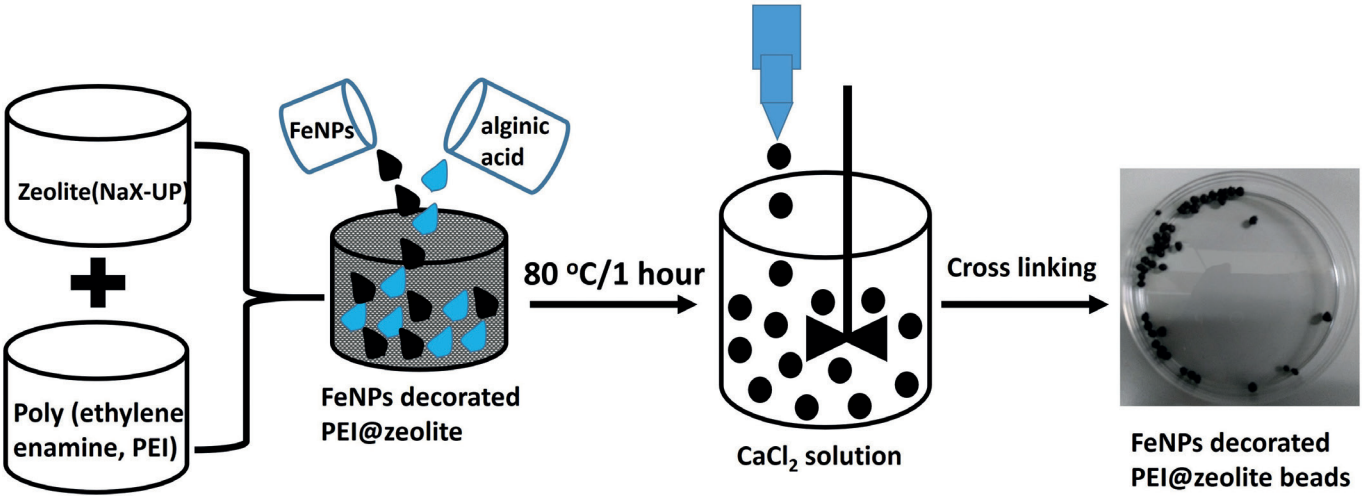

Figure 3. Schematic illustration for preparation of magnetic alginate bead (adsorbent).

adsorbed contaminated (q_e) was calculated from the mass balance equation:

$$q_e = \frac{(C_{initial} - C_e)V}{W} \quad (1)$$

where W and V are the weight (g) of the adsorbent and the volume (L) of supernatant solution, respectively. The removal efficacy (% *RE*) was calculated according to the equation:

$$\%RE = \frac{(C_{initial} - C_{final})}{C_{initial}} \times 100 \quad (2)$$

3. Results and Discussion

3.1. BET surface area

Brunauer-Emmett-Teller (BET) theory was used to measure the surface area of NaX-UP zeolites. It needs to be stated here that this method does not allow the measurement of the surface properties of Fe_3O_4 NPs loaded PEI-NaX-UP zeolites and PEI-NaX-UP zeolite. The BET measurement of NaX-UP zeolite displays a curvilinear pattern in relation to the type IV isotherm, with a distinct H3 ring representing the mesoporous structure (Figure 4). The BJH (Barrett, Joyner, and Halenda) method was exploited to estimate surface area and total pore volume values (Table 2). Nitrogen adsorption-desorption isotherm measurements indicate that the surface area, pore volume, and pore diameter of NaX-UP zeolites were 472 $m^2\ g^{-1}$, 0.13 $cm^3\ g^{-1}$, and 6.5 nm, in sequence (Figure 4).

3.2. Powder XRD

As shown in (Figure 5A, black line), the as synthesized NaX-UP zeolite shows a powder XRD spectra with significant diffraction peaks of 10.1°, 12.0°, 15.5°, 20.3°, 23.4°, 26.8°, 31.2°, 33.7°, 37. 6°, 40.9°, 53.4°, and 57.6°. These result are indicates that NaX-UP zeolites are highly crystalline which have limited amorphous potential, to correlates well with previous studies in the literature (Izidoro et al. 2013; Kunecki et al. 2021; Amoni et al. 2022). The XRD spectra of the as synthesized bare Fe_3O_4 NPs show significant diffraction peaks at 30.3°, 35.7°, 43.2°, 53.7°, 57.2°, and 63.1, corresponding to the (220), (311), (400), (422) and (511) facets of the lattice of cubic Fe_3O_4 NPs (JCPDS No. 019-0629) (Figure 5C, dark blue line) [Santhana Krishna Kumar et al. 2022]. Thus, Fe_3O_4 NPs decorated with PEI-modified NaX-UP zeolites show intense diffraction peaks of 35.8°, 43.5°, 53.7°, 57.4°, and 63.1° corresponding to the cubic Fe_3O_4 NPs (Figure 5D, dark yellow line). This peak position are slightly shifted up and down, indicating more number of Fe_3O_4 NPs decorated on their zeolite surface, which are suggesting that a strong binding interaction between Fe_3O_4 NPs and PEI-modified NaX-UP zeolite [Kunecki et al. 2021; Santhana Krishna Kumar et al. 2022]. In other words, Fe_3O_4 NPs have a great combination on the surface of crystalline behavior of PEI-modified NaX-UP zeolite, and it is noteworthy that the XRD patterns of Fe_3O_4 NPs move somewhat to lower angles after the modification process with the zeolite porous solid support. Moreover, no other contaminating phases were observed from the nano-composites of Fe_3O_4 NPs loaded PEI-modified NaX-UP zeolite, indicating that the combination of PEI-modified NaX-UP zeolites and Fe_3O_4 NPs is well immobilized on their surfaces [Kunecki et al. 2021; Santhana Krishna Kumar et al. 2022].

3.3. SEM-EDS analysis

Field emission scanning electron microscopy (FE-SEM) coupled with elemental (EDS) mapping was further

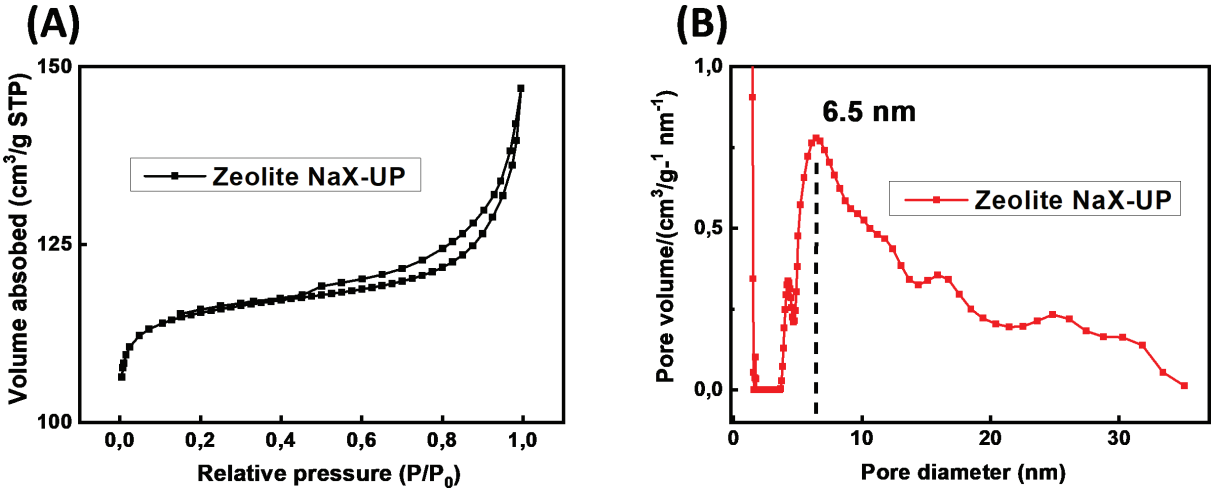

Figure 4. (A) BET adsorption isotherms of NaX-UP zeolites, (B) Pore size distribution of zeolites.

Table 2. Surface area, pore volume and pore diameter of NaX-UP zeolites.

S. No.	S_{BET} ($m^2\ g^{-1}$)	$V_{tot}^{0,99}$ ($cm^3\ g^{-1}$)	V_{mik}^{DR} ($cm^3\ g^{-1}$)	V_{mez}^{BJH} ($cm^3\ g^{-1}$)
1	472.0	0.222	0.176	0.13

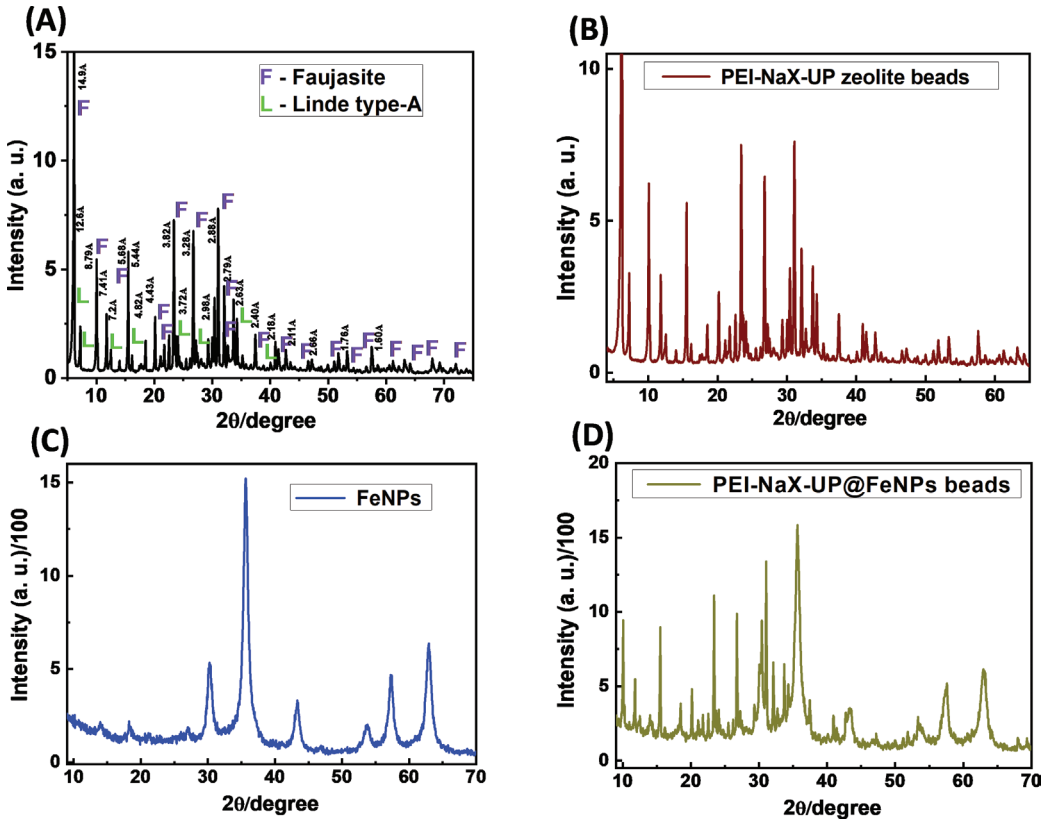

Figure 5. (A, B, C and D) Powder XRD spectra for (A) NaX-UP zeolite, black line (B) PEI-modified NaX-UP zeolite NSs, brown line; (C) bare Fe_3O_4 NPs, navy blue line, (D) Fe_3O_4 NPs decorated PEI-modified NaX-UP zeolite, green line.

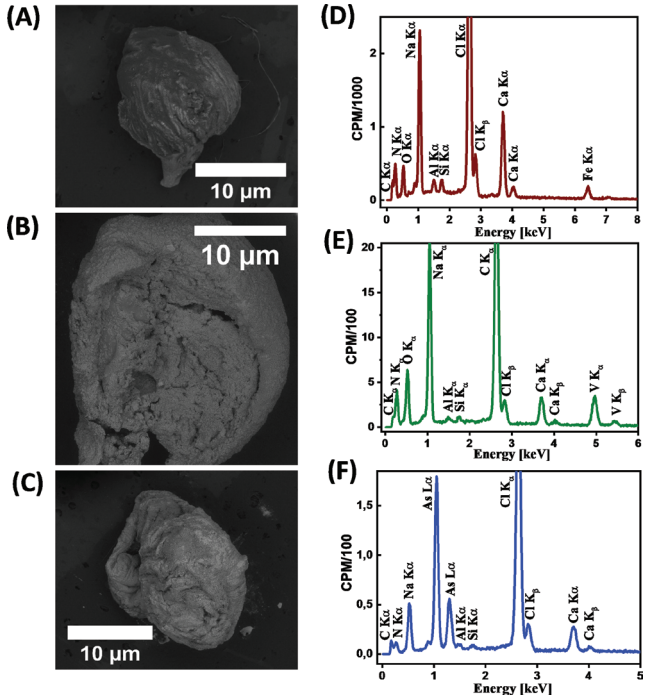

Figure 6. HR-SEM images and EDS spectra of (A) the bare Fe_3O_4 NPs were decorated on their surface of PEI-zeolite NSs alginate bead adsorbent, (B and C) after sorption of As(V) & V(V). From (A, B, C) denoted as HR-SEM images, (D, E, F) EDS spectra.

adapted to demonstrate nano-composite formation, as shown in Figure 6. The as-prepared adsorbent of magnetic alginate bead consists of silicon, alumina, carbon, nitrogen, oxygen and iron, the iron element which arises from the contribution of Fe_3O_4 NPs. These results are strongly recommend that Fe_3O_4 NPs were successfully assembled on the surface of PEI- zeolite NSs, as depicted in (Figure 6D). The above information infers that the as-prepared magnetic alginate bead (adsorbent) provides more defective structure (Figure 6A), which are highly favorable for efficient sorption of As(V) and V(V) are depicted in Figures 6B and 6C. Inspired by this information, we further identified that, after sorption of As(V) and V(V), the existence of these elements from the surface of the adsorbent, as we depicted from EDS spectroscopic studies, were shown in (Figures 6E and F).

3.4. Adsorption Equilibrium

Adsorption equilibrium studies were used to determine the mass of the adsorbent per unit weight and their concentration of As(V) and V(V) at a fixed pH. The q_e value rises sharply while increasing their C_e values correspondingly. This feature indicates that electrostatic attraction dominated for capturing the anionic species of As (V) and V (V) on their surface of adsorbent (Kalidhasan et al. 2012, 2013; Santhana Krishna Kumar et al. 2012, 2013, 2022). Moreover, the plateau portion of the curve signifies that the number of binding sites on the surface of these specified adsorbents is limited for capturing As (V) and V (V) from an aqueous solution as shown in Figures 7A and 7B. Considering that Freundlich and Langmuir's isotherms are frequently applied to evaluate their type of adsorption isotherms, the resultant equilibrium data of these three different type of adsorbents were fitted by two isotherm models, from that Freundlich isotherm model are well fitted as shown in Table 3 regression coefficient are close to 1, these results are demonstrating that the as proposed adsorbents are sufficiently correlating their heterogeneous surface for multilayer sorption of As

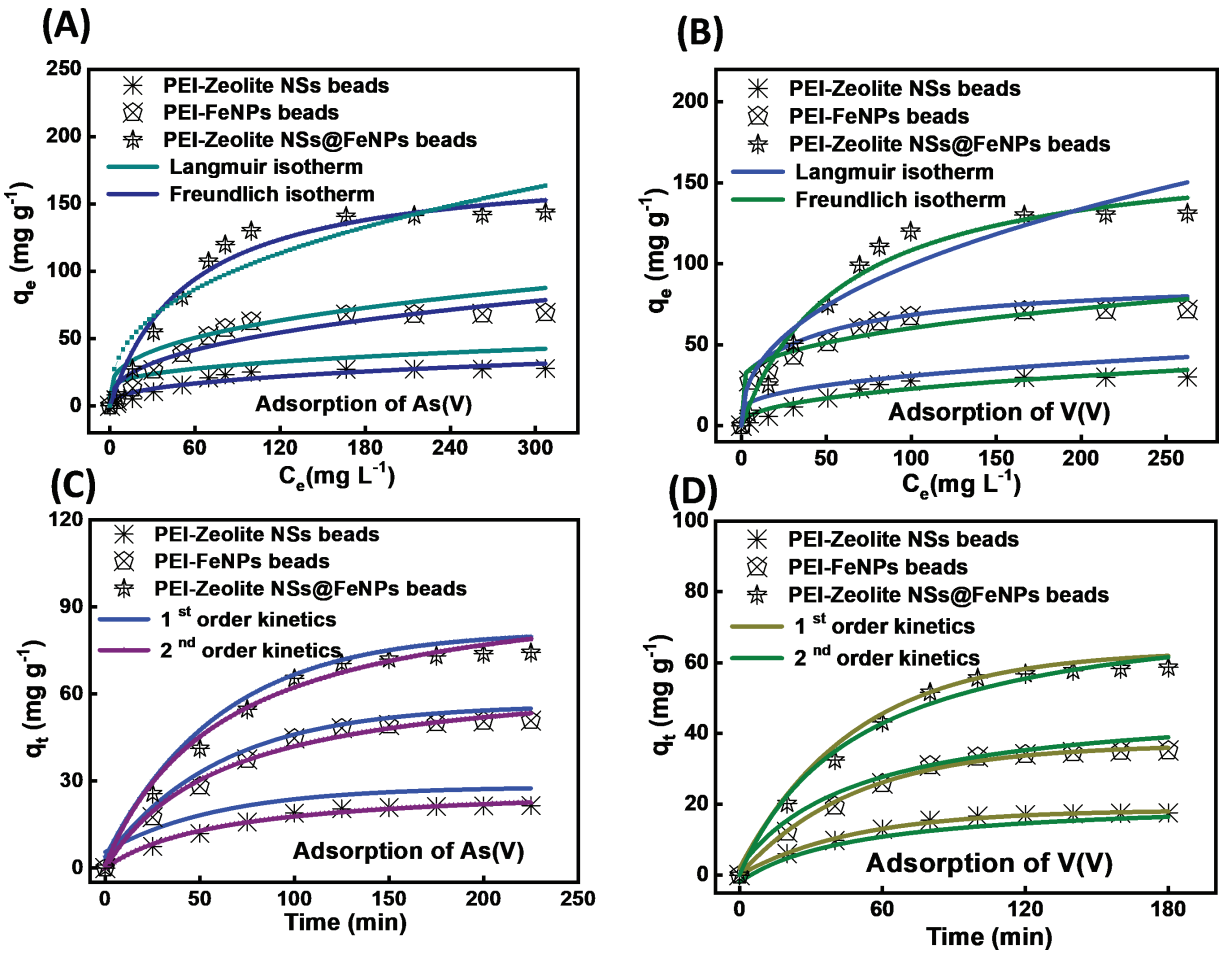

Figure 7. Alginate beads mediated sorption of As(V) and V(V), (A, B) adsorption isotherms modeling of PEI modified NaX-UP zeolite beads, PEI modified Fe_3O_4 NPs beads, and Fe_3O_4 NPs decorated PEI modified NaX-UP zeolite beads for (A) As(V) and (B) V(V); adsorption isotherms modeling fitting with the Freundlich model (A: navy blue line; B: dark green line) and Langmuir model (A: cyan line; B: sky blue line). (C, D) Kinetic sorption curves of the PEI modified NaX-UP zeolite beads, PEI modified Fe_3O_4 NPs beads, and Fe_3O_4 NPs decorated PEI modified NaX-UP zeolite beads for (C) As(V) and (D) V(V), modeling of kinetics sorption curves with the pseudo-first-order kinetics (C: sky blue line; D: dark yellow line) and pseudo-second-order kinetic (C: dark brown line; D: dark green line). (A, B) Beads-mediated sorption of As (V) and V(V), (C, D) Kinetic sorption curves of As (V) and V(V), PEI-zeolite NSs modified alginate beads, bare Fe_3O_4 NPs modified alginate beads, and bare Fe_3O_4 NPs decorated on their surface of PEI-zeolite NSs modified alginate beads (1.0 g) were incubated with various concentration of As(V) and V(V) at pH 4.5 for isotherm studies (A, B) and (C, D) the alginate beads were incubated with 50 mg mL^{-1} of As(V) and V(V) various time interval from 0-240 min at 298 K.

(V) and V (V) (Kalidhasan et al. 2012, 2013; Santhana Krishna Kumar et al. 2012, 2013, 2022). Additionally, the maximum adsorption capacity (q_m) value was estimated to be 163 mg g^{-1} for As (V), similarly 151 mg g^{-1} for V (V) according to the following equation 3 (Santhana Krishna Kumar et al. 2022),

$$q_e = \frac{q_m b C_e}{1 + b C_e} \quad (3)$$

Table 3, displays the calculated values of q_e (mg g^{-1}), C_e (mg L^{-1}), q_m (mg g^{-1}), and b (L mg^{-1}; adsorption energy). It's worth emphasizing that the q_e values of PEI-zeolite NSs modified alginate beads was estimated to be [(35 mg g^{-1} for As(V), 38 mg g^{-1} for V(V)], bare Fe_3O_4 NPs modified alginate beads were estimated to be [(88 mg g^{-1} for As(V), 53 mg g^{-1} for V(V)], similarly the-as prepared Fe_3O_4 NPs decorated PEI-modified zeolite NSs alginate beads were estimated to be [(163 mg g^{-1} for As(V), 151 mg g^{-1} for V(V)] respectively. Thus, the assembly of Fe_3O_4 NPs decorated on their surface of PEI-zeolite NSs modified alginate beads can improve their sorption efficiency for capturing As (V) and V(V) (Kalidhasan et al. 2012; Santhana Krishna Kumar et al. 2013; (Kalidhasan et al. 2013; Santhana Krishna Kumar et al. 2012, 2022). However, exhibiting a better q_e value than most of the previously published nano-materials as shown in Tables 4 and 5.

By contrast, the Langmuir isotherm model somewhat offers not the best fit with the Freundlich isotherm model. We recommend that, the as-prepared adsorbents contain an unlimited number of active sites have equal affinities towards to sorption of As(V) and V(V). The Freundlich isotherm parameters were obtained according to the following equation 4:

$$q_e = K_F C_e^{1/n} \quad (4)$$

where K_F [(mg g^{-1}) (L mg^{-1})$^{1/n}$] are Freundlich constant corresponding to their adsorption capacity, and n is denoted to be adsorption intensity. The n value is 2.1 for As (V), and 1.9 for V (V), the as-prepared adsorbent

Table 3. Adsorption isotherm parameters for uptake of Arsenic(V) and Vanadium(V).

Sl. No.	Adsorbent	Isotherm	Characteristic values	Uptake of As(V)	Uptake of V(V)
1	PEI-modified zeolite beads	Langmuir	q_m (mg g^{-1})	35.4	38.9
			b (L mg^{-1})	0.014	0.014
			R_L	0.69	0.69
			Adj. R^2	0.96	0.96
2	PEI-modified zeolite beads	Freundlich	K_F (mg $^{1-1/n}$ g^{-1} $L^{1/n}$)	0.40	0.44
			n	1.08	1.08
			Adj R^2	0.98	0.98
3	PEI-modified Fe_3O_4 beads	Freundlich	K_F (mg $^{1-1/n}$ g^{-1} $L^{1/n}$)	1.008	0.68
			n	1.08	1.02
			Adj R^2	0.98	0.98
4	PEI-modified Fe_3O_4 beads	Langmuir	q_m (mg g^{-1})	88.4	53.1
			b (L mg^{-1})	0.01	0.02
			R_L	0.57	0.30
			Adj. R^2	0.96	0.96
5	Fe_3O_4 decorated PEI-modified zeolite beads	Langmuir	q_m (mg g^{-1})	163.9	151.5
			b (L mg^{-1})	0.02	0.02
			R_L	0.25	0.25
			Adj. R^2	0.96	0.96
6	Fe_3O_4 decorated PEI-modified zeolite beads	Freundlich	K_F (mg $^{1-1/n}$ g^{-1} $L^{1/n}$)	2.09	1.93
			n	1.08	1.08
			Adj R^2	0.98	0.98

Table 4. Arsenic (V) adsorption capacity of various adsorbents reported in the literature.

Adsorption material	pH	q_m (mg g^{-1})	Reference
Alginate@Iron-zirconium@Zeolite W	2.0	42.3	Abdellaoui et al. 2021
Chitosan-coated Na–X zeolite	2.0	63.2	Han et al. 2019
Zeolite@nanoscale zero-valent iron	3.0	38.2	Suazo-Hernandez et al. 2019
Na-X zeolite derived from cola fly ash	2.14	27.7	Yang et al. 2019
Nanozero valent iron (NZVI) loaded on zeolite 5A	4-12	72.0	Yang et al. 2022.
β-cyclodextrin modified graphene oxide @ Fe_3O_4 NPs	4-7.2	99.5	Santhana Krishna Kumar et al. 2017
Iron oxide (hydr) modified zeolite	3.5	1.69	Nekhunguni et al. 2017
Ferric hydroxide microcapsule-loaded alginate beads	-	3.80	Sarkar et al. 2010
Calcium alginate beads@methionine magnetic NPs	7-7.5	6.6	Lilhare et al. 2021
Aluminum(III) exchange synthetic zeolite	3-10	10.5	Xu et al. 2002
Fe-treated synthetic zeolite	-	22.5	Dousova et al. 2006
Cerium(III) exchange synthetic zeolite	-	23.4	Haron et al. 2008
Synthetic zeolites	3.2	35.8	Chutia et al. 2009
PEI-modified zeolite beads	5-7.5	35.4	This study
PEI-modified Fe_3O_4 beads	5-7.5	88.4	This study
Fe_3O_4 decorated PEI-modified zeolite beads	5-7.5	163.9	This study

(Fe_3O_4 NPs decorated PEI-modified zeolite NSs alginate beads), which is larger than 1.0, suggesting that their specific interaction with As(V) and V(V) (Santhana Krishna Kumar et al. 2022).

$$K_F = \frac{q_m}{C_0^{1/n}} \quad (5)$$

In addition, in each case of three different types of adsorbents, the q_t values gradually increase with contact time further that could achieve a saturation level after 100 min. The as-prepared adsorbents can efficiently capture a large amount of As(V) and V(V). This fast sorption time reflects that the as-prepared magnetic alginate bead (Fe_3O_4 NPs decorated PEI-modified zeolite NSs alginate beads) have a large surface area for interacting with more amount of anionic species are As(V) and V(V) (Kalidhasan et al. 2012, 2013; Santhana Krishna Kumar et al. 2012, 2013, 2022).

Additionally, the adsorption time is relatively shorter than that of previously published nanomaterials as shown in Tables 6 and 7. It's well assumed that the assembly of Fe_3O_4 NPs decorated on their porous zeolite adsorbent could further shorten their adsorption time for As(V) and V(V) (Santhana Krishna Kumar et al. 2022). The pseudo-first-order rate constant (k_1) and pseudo-second-order rate constant (k_2) were

Table 5. Vanadium adsorption capacity of various adsorbents reported in the literature.

Adsorption material	pH	q_m (mg g^{-1})	Reference
LDH supported nanoscale zero valent iron	3.0	93.7	Kong et al. 2020
Magnetic zeolite–polypyrrole composite	4-5	74.9	Mthombeni et al. 2016
Syrian natural zeolite	6.0	40.0	Salman et al. 2017
Goethite	4-8	8.2	Zhu et al. 2020
Clinoptilolite modified polypyrrole and iron oxide NPs	4.5	12.0	Mthombeni et al. 2018
Synthesised zero-valent iron modified kaloin	5.0	15.0	Bello et al. 2019
Octylamine functionalized magnetite NPs	3.2	25.7	Parijaee et al. 2014
Zeolite A	4.5	30.0	Mahmood et al. 2019
PGTFS-$NH_3^+Cl^-$	6.0	45.9	Anirudhan et al. 2010
Biochar stabilized nano zero-valent iron	2-10	48.5	Fan et al. 2020
Metal (hydr)oxide adsorbents	3-4	111.1	Naeem et al. 2007
PEI-modified zeolite beads	5-7.5	38.9	This study
PEI-modified Fe_3O_4 beads	5-7.5	53.1	This study
Fe_3O_4 decorated PEI-modified zeolite beads	5-7.5	151.5	This study

Table 6. Arsenic (V) equilibrium kinetics sorption, adsorption capacity of various adsorbents reported in the literature.

Adsorption material	Equilibrium kinetics (Time in min)	q_m (mg g^{-1})	Reference
Chitosan-coated Na–X zeolite	720 min	63.2	Han et al. 2019
Na-X zeolite derived from cola fly ash	120 min	27.7	Yang et al. 2019
Iron oxide (hydr) modified zeolite	90 min	1.69	Nekhunguni et al. 2017
Calcium alginate beads@Methionine magnetic NPs	110 min	6.6	Lilhare et al. 2021
Aluminum(III) exchange synthetic zeolite	960 min	10.5	Xu et al. 2002
Synthetic zeolites	100 min	35.8	Chutia et al. 2009
PEI-modified zeolite beads	100 min	35.4	This study
PEI-modified Fe_3O_4 beads	100 min	88.4	This study
Fe_3O_4 decorated PEI-modified zeolite beads	100 min	163.9	This study

Table 7. Vanadium equilibrium kinetics sorption, adsorption capacity of various adsorbents reported in the literature.

Adsorption material	Equilibrium kinetics (Time in hours)	q_m (mg g^{-1})	Ref
Magnetic zeolite–polypyrrole composite	4 hours	74.9	Mthombeni et al. 2016
Goethite	12 hours	8.2	Zhu et al. 2020
Clinoptilolite modified polypyrrole and iron NPs	14 hours	12.0	Mthombeni et al. 2018
Synthesised zero-valent iron modified kaloin	2 hours	15.0	Bello et al. 2019
PGTFS-$NH_3^+Cl^-$	4 hours	45.9	Anirudhan et al. 2010
PEI-modified zeolite beads	1.5 hours	38.9	This study
PEI-modified Fe_3O_4 beads	1.5 hours	53.1	This study
Fe_3O_4 decorated PEI-modified zeolite beads	1.5 hours	151.5	This study

separately calculated by the following expressions 6 and 7:

$$q_t = q_e\left(1 - e^{-K_1 t}\right) \quad (6)$$

$$q_t = \frac{k_2 q_e^2}{1 + k_2 q_e t} \quad (7)$$

The kinetic data of the three different types of adsorbents, which are following a pseudo-second-order model as shown in Table 8**,** implies that chemisorption dominates their adsorption process. These findings are consistent with the above data. These information's are well related to the experimental evidence of effect of solution pH and the removal efficiency of As(V) and V(V) against their adsorbent. It's recommended that, the chemisorption of As(V) and V(V) on the surface of adsorbent (Fe_3O_4 NPs decorated PEI modified zeolite NSs alginate bead), which involves two main sorption processes: (1) exterior mass transfer whereas anionic species of As(V) and V(V) can diffuse from the bulk solution to the surface of adsorbent; (2) chemisorption of As(V) and V(V) species penetrates intra-particle pores and then strongly binding with their active sites of adsorbent (Santhana Krishna Kumar et al. 2022).

3.5. Thermodynamics of adsorption

Thermodynamic studies are an important parameter to ascertain the feasibility and nature of the

Table 8. Adsorption kinetics for uptake of Arsenic(V) and Vanadium(V)

Sl. No	Adsorbent	Order of kinetics	Characteristic values	Uptake of As(V)	Uptake of Vanadium(V)
1	PEI-modified zeolite beads	Pseudo first order	q_e (mg g^{-1})	1.36	1.28
			k_1	0.007	0.018
			Adj. R^2	0.92	0.94
2	PEI-modified zeolite beads	Pseudo second order	q_e (mg g^{-1})	28.4	23.2
			k_2	0.0005	0.0008
			Adj R^2	0.98	0.98
3	PEI-modified Fe_3O_4 beads	Pseudo second order	q_e (mg g^{-1})	67.1	46.5
			k_2	0.0002	0.0004
			Adj R^2	0.98	0.98
4	PEI-modified Fe_3O_4 beads	Pseudo first order	q_e (mg g^{-1})	1.66	1.58
			k_1	0.016	0.019
			Adj. R^2	0.96	0.94
5	Fe_3O_4 decorated PEI-modified zeolite beads	Pseudo first order	q_e (mg g^{-1})	1.86	1.72
			k_1	0.014	0.02
			Adj. R^2	0.94	0.94
6	Fe_3O_4 decorated PEI-modified zeolite beads	Pseudo second order	q_e (mg g^{-1})	99.0	77.5
			k_2	0.0001	0.0002
			Adj R^2	0.98	0.98

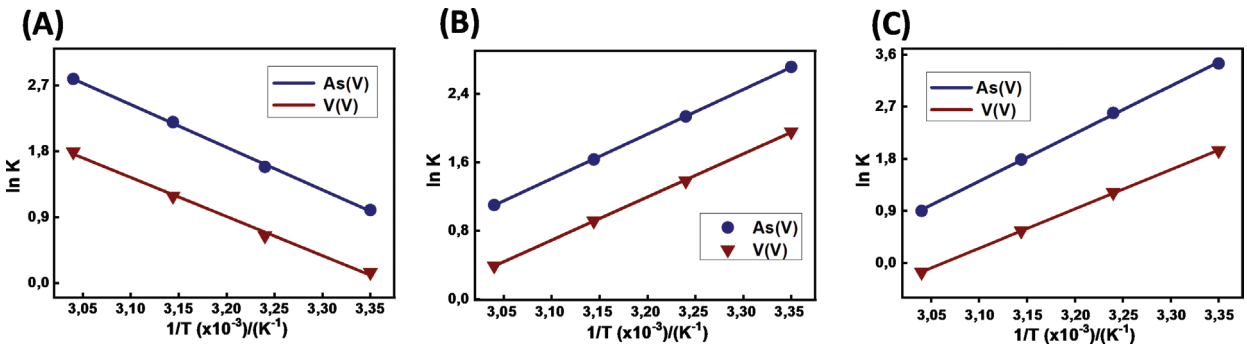

Figure 8. (A, B, C) Van't Hoff plot for the adsorption of As (V) and V (V) on the (A) PEI-zeolite NSs modified alginate beads, (B) Fe_3O_4 NPs modified alginate beads, and (C) Fe_3O_4 NPs decorated PEI modified zeolite NSs alginate beads. (A-C) The beads-related nanomaterials (1.0 g) were incubated with 50 mg mL^{-1} of As (V) and V (V) at 298, 308, 318, and 328 K for 0-240 min under pH 7.0 conditions.

adsorption process. Therefore, the temperature effect was examined in the range of 298-328 K, and the obtained results are depicted in (Figure 8). These thermodynamic parameters, namely, standard free energy (ΔG^0), standard enthalpy (ΔH^0), and standard entropy (ΔS^0), changes, and these changes were determined at various temperatures; thermodynamic studies which gives an equilibrium constants, ΔH^0 and ΔS^0, were obtained from the slope and intercept of van't Hoff plot from lnK against 1/T (see in Figures 8B and 8C), for an exothermic reaction slope is positive, and the equilibrium constants are increases with temperature increases (Kalidhasan et al. 2012, 2013; Santhana Krishna Kumar et al. 2013, 2022).

$$\Delta G^0 = -RT\ln K \tag{8}$$

$$\ln K = \frac{-\Delta H^0}{RT} + \frac{\Delta S^0}{R} \tag{9}$$

Where R is the gas constant (J K^{-1} mol^{-1}), T is the temperature in (Kelvin), and K is obtained from the ratio of the concentration of adsorbate (As(V) and V(V)) in the solid and liquid phases respectively, broadly speaking, K > 1 implies that the adsorption is effective and spontaneous at a given temperature. The adsorption gradually increases at a higher temperature, and this result reveals that adsorbate–adsorbent interaction is feasible at higher temperatures, indicating that higher temperature is more favourable to the adsorption process (PEI-Fe_3O_4 NPs beads and Fe_3O_4 NPs loaded PEI-zeolite NSs beads), the adsorption of As(V) and V(V) gradually increases at a higher temperature. This attraction is more efficient at higher temperatures because their obtained ΔG^0 values decreases along with temperature (Table 9). The negative free energy (ΔG^0) values further confirm the effectiveness of electrostatic interaction (ion-pair interaction) between the heavy metals and adsorbent surface (Kalidhasan et al. 2012, 2013; Santhana Krishna Kumar et al. 2013, 2022). Therefore, a higher temperature indicates that more efficiently to adsorb the inorganic pollutants. Here, the bonding between the adsorbent (PEI-Fe_3O_4 NPs beads and Fe_3O_4 NPs loaded PEI-zeolite NSs beads) and adsorbate is mainly due to ion-pair interaction.

Table 9. Adsorption of thermodynamics for uptake of As(V) and V(V).

S. No.	Adsorbent	Uptake of metals	ΔS^0 J mol^{-1}	ΔH^0 KJ mol^{-1}	ΔG^0 KJ mol^{-1}			
					298K	308K	318K	328K
1	PEI-Zeolite NSs beads	As(V)	145.7	42.5	−2.1245	−3.9625	−5.2465	−6.8752
		V(V)	124.8	39.1	−1.4523	−2.2754	−3.1465	−4.1254
2	PEI-Fe_3O_4 NPs beads	As(V)	−121.3	−37.2	−6.8875	−5.2354	4.26548	−2.1256
		V(V)	−91.3	−26.7	−4.2810	−3.8965	−2.23689	−1.4689
3	PEI-Zeolite NSs@ Fe_3O_4 NPs beads	As(V)	−163.1	−54.8	−8.3567	−7.3658	−5.2136	−2.8969
		V(V)	−126.4	−50.3	−5.1209	−3.6875	−1.4232	−2.0256

Furthermore, the enthalpy change (***ΔH***^{0}) was negative, confirming that, the exothermic nature of adsorption. The magnitude of ***ΔH***^{0} gives information about the mechanism of adsorption process; in physical sorption, the process is fast and usually reversible due to the small energy requirement. London requires energies from 4 to 8 kJ mol^{-1}, and Van der Waals interactions are needed from 8 to 40 kJ mol^{-1}. In contrast, enthalpy associated with chemical sorption is about 40 kJ mol^{-1}, a value that has been recognized in the literature as the transition boundary between both types of sorption processes (Kalidhasan et al. 2012, 2013; Santhana Krishna Kumar et al. 2012, 2013). For our current studies, the calculated ΔH^0 values for As (V) and V (V) sorption were lower than that of 4 kJ mol^{-1}, indicating that weak interaction between the adsorbate and adsorbents were observed throughout our studies (Table 9).

For an endothermic reaction, the slope is positive (see Figure 8A) and the equilibrium constant (lnK) decreases with increasing temperature, which reflects the free energy values are obtained at lower temperatures, and lower temperatures favor the adsorption process (PEI-zeolite NSs alginate beads), as can be seen from these values (see Table 9). Thus, the bonding process decreases with increasing temperature. In the case of PEI-zeolite NSs alginate beads, the adsorption is influenced by the physisorption. The literature reports that physisorption initially increases as more metal ions gain enough energy for strong bonding. Further temperature increase leads to a break in the binding between the metal ions and the adsorbent, reducing their adsorption behavior at higher temperatures. Thus, higher temperatures are unfavorable for the adsorption process, indicating that adsorption favors 298 K, as shown by the ΔG^0 values are obtained at different temperatures (see Table 9). In addition, the enthalpy change (ΔH^0) is positive, confirming the endothermic nature of the adsorption (see Table 9) (Kalidhasan et al. 2012, 2013; Santhana Krishna Kumar et al. 2012, 2013, 2022).

4. Conclusion

Zeolite (NaX-UP) was successfully prepared from coal fly ash (CFA) via fusion-hydrothermal treatment. The as-prepared magnetic beads exhibit several functional groups on their surface of adsorbent (e.g., -N, -NH, -NH_2, and Fe-OH). These merits are allow that the-as prepared adsorbent could further enhance their electrostatic attraction with negatively charged As(V) species are $H_2AsO_4^-$, $HAsO_4^{2-}$ AsO_4^{3-} besides V(V) species are $H_2VO_4^-$ and HVO_4^{2-} which are beneficial to uptake more than 90% of sorption were achieved from an aqueous solution in wide pH range. The as-prepared adsorbent exhibited superior adsorption activity toward their sorption of As(V) and V(V) in an aqueous solution. The kinetics sorption of As(V) and V(V) was reached within 100 mins for more than 90% removal, which is relatively faster sorption kinetics as compared with earlier literature evidence and its highly correlating with pseudo-second-order kinetics model. The experimental studies are well suited and associated with Freundlich adsorption isotherm, indicating that the multilayers of adsorption process are more prominent. The maximum adsorption efficiencies are determined to be As(V) and V(V), 163 and 151 mg g^{-1}, respectively. More specifically, the adsorption ability for As(V) and V(V) is quite more significant and superior to those earlier reported adsorbent materials. A possible mechanism for As(V) and V(V) adsorption was proposed to be a combination of electrostatic interaction, and surface complexation is mostly predominant. Under an external magnetic field, the separation techniques are straightforward and rapid.

Acknowledgements

We want to thank the financial support of this study, and also, this research was funded by the POIR.04.04.00-00-14E6/18-00. Project is carried out within the TEAM-NET programme of the Foundation for Polish Science, co-financed by the European Union under the European Regional Development Fund.

Author Contributions

Eugeniusz Swistun: Formal analysis, Data curation, **Maciej Sobczyk:** Data curation, **A. Santhana Krishna Kumar:** Conceptualization, Methodology, Data curation, Investigation, Formal analysis, Writing-original draft, **Wei Lung Tseng:** Investigation, Writing-review & editing. **Tomasz Bajda:** Resources, Funding acquisition, Writing-review & editing.

Competing Interests

The authors declare no competing interests.

Data Availability

The corresponding author's data supporting this study's findings are available upon reasonable request.

References

Abdellaoui, Y., El Ibrahimi, B., Oualid, H. A., Kassab, Z., Quintal-Franco, C., Giacoman-Vallejos, G., & Gamero-Melo, P. (2021). Iron-zirconium microwave-assisted modification of small-pore zeolite W and its alginate composites for enhanced aqueous removal of As(V) ions: Experimental and theoretical studies. *Chemical Engineering Journal, 421,* 129909. DOI:10.1016/j.cej.2021.129909.

Amoni, B. C., Freitas, A. D. L., Bessa, R. A., Oliveira, C. P., Bastos-Neto, M., Azevedo, D. C. S., Lucena, S. M. P., Sasaki, J. M., Soares, J. B., Soares, S. A., & Loiola, A. R. (2022). Effect of coal fly ash treatments on the synthesis of high-quality zeolite A as a potential additive for warm mix asphalt. *Materials Chemistry and Physics, 275,* 125197. DOI:10.1016/j.matchemphys.2021.125197.

Anirudhan, T. S., Radhakrishnan, P. G. (2010). Adsorptive performance of an amine-functionalized poly(hydroxyethylmethacrylate)-grafted tamarind fruit shell for vanadium (V) removal from aqueous solutions. *Chemical Engineering Journal* 165, 142–150. DOI: 10.1016/j.cej.2010.09.005.

Bello, A., Leiviskä, T., Zhang, R., Tanskanen, J., Maziarz, P., Matusik, J., Bhatnagar, A. (2019). Synthesis of zerovalent iron from water treatment residue as a conjugate with kaolin and its application for vanadium removal. *Journal of Hazardous Materials, 374,* 372–381. DOI: 10.1016/j.jhazmat.2019.04.056.

Chutia, P., Kato, S., Kojima, T., Satokawa, S. (2009). Arsenic adsorption from aqueous solution on synthetic zeolites. *Journal of Hazardous Materials, 162*, 440–447. DOI:

Dousova, B., Grygar, T., Martaus, A., Fuitova, L., Kolousek, D., Machovic, V. (2006). Sorption of As(V) on alumino-silicates treated with Fe(II) nanoparticles. *Journal of Colloid and Interface Science, 302,* 424–431. DOI: 10.1016/j.jcis.2006.06.054.

Fan, C.-G., Chen, N., Qin, J., Yang, Y.-Q., Feng, C-P., Li, M., Gao, Y. (2020). Biochar stabilized nano zero-valent iron and its removal performance and mechanism of pentavalent vanadium (V). *Colloids and Surfaces A, 599,* 124882. DOI: 10.1016/j.colsurfa.2020.124882.

Han, C., Yang, T., Liu, H., Yang, L., & Luo, Y. (2019). Characterizations and mechanisms for synthesis of chitosan-coated Na-X zeolite from fly ash and As(V) adsorption study. *Environmental Science and Pollution Research, 26,* 10106-10116. DOI: 10.1007/s11356-019-04466-x.

Haron, Mhd. J., Rahim, F. Ab., Abdullah, A.H., Hussein, M.Z., Kassim, A. (2008). Sorption removal of arsenic by cerium-exchanged zeolite P. *Material Science Engineering part B, 149,* 204-208. DOI: 10.1016/j.mseb.2007.11.028.

Izidoro, J., Fungaro, D., Abbott, J., & Wang, S. (2013). Synthesis of zeolites X and A from fly ashes for cadmium and zinc removal from aqueous solutions in single and binary ion systems. *Fuel, 103,* 827-834. DOI:10.1016/j.fuel.2012.07.060.

Kalidhasan, S., Gupta, P. A., Cholleti, V. R., Santhana Krishna Kumar, A., Rajesh, V., & Rajesh, N. (2012). Microwave assisted solvent free green preparation and physicochemical characterization of surfactant-anchored cellulose and its relevance toward the effective adsorption of chromium. *Journal of Colloid and Interface Science, 372,* 88-98. DOI:10.1016/j.jcis.2012.01.013.

Kalidhasan, S., Santhana Krishna Kumar, A. Rajesh, V. & Rajesh, N. (2013). Enhanced adsorption of hexavalent chromium arising out of an admirable interaction between a synthetic polymer and an ionic liquid. *Chemical Engineering Journal, 222,* 454-463. DOI:10.1016/j.cej.2013.02.083.

Kong, X., Chen, J., Tang, Y., Lv, Y., Chen, T., & Wang, H. (2020). Enhanced removal of vanadium (V) from groundwater by layered double hydroxide-supported nano-scale zero-valent iron. *Journal of Hazardous Materials, 392,* 122392. DOI: 10.1016/j.jhazmat.2020.122392.

Kunecki, P., Panek, R., & Wdowin, M. et al. (2021). Influence of the fly ash fraction after grinding process on the hydrothermal synthesis efficiency of Na-A, Na-P1, Na-X and sodalite zeolite types. *International Journal of Coal Science & Technology, 8,* 291-311. DOI:10.1007/s40789-020-00332-1.

Lilhare, S., Mathew, S. B., Singh, A. K., Carabineiro, S. A. C. (2021). Calcium alginate beads with entrapped iron oxide magnetic nanoparticles functionalized with methionine-a versatile adsorbent for arsenic removal. *Nanomaterials, 11,* 1345-1366. DOI: 10.3390/nano11051345.

Mahmood, L. H., Abid, M. F. (2020). Dmetallization of Iraqi crude oil by using zeolite A. *Indian Chemical Engineer, 62*, 92-102. DOI: 10.1080/00194506.2019.1641432.

Mthombeni, N. H., Mbakop, S., Ochieng, A., & Onyango, M.S. (2016). Vanadium(V) adsorption isotherms and kinetics using poly-pyrrole coated magnetized natural zeolite. *Journal of the Taiwan Institute of Chemical Engineers, 66,* 172-180. DOI:10.1016/j.jtice.2016.06.016.

Mthombeni, N. H., Mbakop, S., Ochieng, A., & Onyango, M. S. (2018). Adsorptive removal of V(V) ions using clinoptilolite modified with polypyrrole and iron oxide nanoparticles in column studies. *MRS Advances, 3,* 2119-2127. DOI:10.1557/adv.2018.229.

Naeem, A., Westerhoff, P., Mustafa, S. (2007). Vanadium removal by metal (hydr) oxide adsorbents. *Water Research, 41,* 1596-1602. DOI: 10.1016/j.watres.2007.01.002.

Nekhunguni, P.M., Tavengwa, N.T., Tutu, H. (2017). Investigation of As(V) removal from acid mine drainage by iron (hydr) oxide modified zeolite. *Journal of* Environmental Management, *197,* 550–558. DOI: 10.1016/j.jenvman.2017.04.038.

Parijaee, M., Noaparast, M., Saberyan, K., Shafaie-Tonkaboni, S. Z. (2014). Adsorption of vanadium (V) from acidic solutions by using octylamine functionalized magnetite nanoparticles as a novel adsorbent. *Korean Journal Chemical Engineering, 31,* 2237-2244. DOI: 10.1007/s11814-014-0179-z.

Santhana Krishna Kumar, A., Kalidhasan, S., Rajesh, V., & Rajesh, N. (2012). A meticulous study on the adsorption of mercury as tetrachloromercurate (II) anion with tri-octylamine modified sodium montmorillonite and its application to a coal fly ash sample. *Industrial & Engineering Chemistry Research, 51,* 11312-11327. DOI:10.1021/ie3008693.

Santhana Krishna Kumar, A., Barathi, M., Puvvada, S., & Rajesh, N. (2013). Microwave assisted preparation of glycidyl methacrylate grafted cellulose adsorbent for the effective adsorption of mercury from a coal fly ash sample. *Journal of Environmental Chemical Engineering, 1,* 1359-1367. DOI:10.1016/j.jece.2013.10.004.

Santhana Krishna Kumar, A., Warchol, J., Matusik, J., Tseng, W.-L., Rajesh, N., Bajda, T. (2022). Heavy metal and organic dye removal via a hybrid porous hexagonal boron nitride-based magnetic aerogel. *npj Clean Water, 5,* 24. DOI:10.1038/s41545-022-00175-0.

Santhana Krishna Kumar, A. & Jiang, S.-J. (2017). Synthesis of magnetically separable and recyclable magnetic nanoparticles decorated with β-cyclodextrin functionalized graphene oxide an excellent adsorption of As(V)/(III). *Journal of Molecular Liquids, 237,* 387-401. DOI:10.1016/j.molliq.2017.04.093.

Salehi, S., Alijani, S., & Anbia, M. (2020). Enhanced adsorption properties of zirconium modified chitosan-zeolite nano-composites for vanadium ion removal. *International Journal of Biological Macromolecules, 164,* 105-120. DOI:10.1016/j.ijbiomac.2020.07.055.

Salman, H., Shaheen, H., Abbas, G., & Khalouf, N. (2017). Use of Syrian natural zeolite for heavy metals removal from industrial waste water: Factors and mechanism. *Journal of Entomology and Zoology Studies, 5,* 452-461.

Sarkar, P., Pal, P., Bhattacharyay, D., Banerjee, S. (2010). Removal of arsenic from drinking water by ferric hydroxide microcapsule-loaded alginate beads in packed adsorption column. *Journal of Environmental Science Health Part A, 45,* 1750–1757. DOI: 10.1080/10934529.2010.513267.

Suazo-Hernandez, J., Sepúlveda, P., Manquian-Cerda, K., Ramírez-Tagle, R., Rubio, M. A., Bolan, N., Sarkar, B., & Arancibia-Miranda, N. (2019). Synthesis and characterization of zeolite-based composites functionalized with nanoscale zero-valent iron for removing arsenic in the presence of selenium from water. *Journal of Hazardous Materials, 373,* 810-819. DOI: 10.1016/j.jhazmat.2019.03.125.

Xu, Y.-H., Nakajima, T., Ohki, A. (2002). Adsorption and removal of arsenic(V) from drinking water by aluminum-loaded shirasu-zeolite. *Journal of Hazardous Materials B, 92,* 275–287. DOI: 10.1016/S0304-3894(02)00020-1.

Yang, L.-Y., Gao, M.-D., Wei, T., & Nagasaka, T. (2022). Synergistic removal of As(V) from aqueous solution by nano-zero valent iron loaded with zeolite 5A synthesized from fly ash. *Journal of Hazardous Materials, 424,* 127428. DOI:10.1016/j.jhazmat.2021.127428.

Yang, T., Han, C.-Y., Liu, H., Yang, L., Liu, D.-K., Tang, J., & Luo, Y.-M. (2019). Synthesis of Na-X zeolite from low aluminum coal fly ash: Characterization and high efficient As(V) removal. *Advanced Powder Technology, 30,* 199-206. DOI:10.1016/j.apt.2018.10.023.

Zhu, H-W., Xiao, X., Guo, Z-H., Peng, C., Wang, X. H., Yang, A. (2020). Characteristics and behavior of vanadium (V) adsorption on goethite and birnessite, *Environmental Earth Science, 79,* 240-249. DOI: 10.1016/j.jhazmat.2008.05.061.

Received: 07 Feb 2023
Accepted: 30 May 2023
Handling Editor: Abigail Barker